

An Overview of the Nadir Sensor and Algorithms for the NPOESS Ozone Mapping and Profiler Suite (OMPS)

J. V. Rodriguez*^a, C. J. Seftor^b, C. G. Wellemeyer^c and K. Chance^d

^aBall Aerospace & Technologies Corp.; ^bRaytheon Information Technology and Scientific Services; ^cScience Systems and Applications, inc; ^dHarvard-Smithsonian Center for Astrophysics

ABSTRACT

The Ozone Mapping and Profiler Suite (OMPS) nadir sensor and algorithms for the United States National Polar-orbiting Operational Environmental Satellite System (NPOESS) comprise a system to map ozone total column globally in 24 hours and to measure the altitude distribution of ozone in the upper stratosphere (30-50 km). The sensor consists of a wide field (110 degree) telescope and two spectrometers: an imager covering 300 to 380 nm with a 50 km nadir footprint for mapping total column ozone across a 2800 km swath, and a 250 to 310 nm spectrometer with a single 250 km footprint to provide ozone profile data with SBUV/2 heritage. Both spectrometers provide 1 nm resolution (full-width at half-maximum, FWHM) spectra. The sensitivity of the OMPS total column algorithm to sensor random and systematic errors is analyzed, and a preliminary evaluation of the potential for deriving concentrations of other trace gases from the calibrated spectral radiances is provided.

Keywords: NPOESS, OMPS, ozone column, ozone profile

1. INTRODUCTION

One of the requirements of the National Polar-orbiting Operational Environmental Satellite System (NPOESS) is to measure ozone total column and profile, both for climate monitoring and as inputs into future numerical weather prediction models^{1,2}. The Ozone Mapping and Profiler Suite (OMPS) sensor and algorithm system is designed to meet this requirement. The OMPS flight hardware includes a nadir backscatter ultraviolet sensor³ comprised of a wide-field pushbroom telescope and two spectrometers, one to measure total column and the other to provide information on the altitude distribution of ozone in the upper stratosphere (30-50 km). The total column spectrometer and algorithms fulfill the requirement to provide a new global map of ozone column within 24 hours, like the Total Ozone Mapping Spectrometer (TOMS) series of instruments, but with significantly improved ozone accuracy and precision⁴. Although the ozone profiling requirements are satisfied by the limb sensor⁵, the nadir profile spectrometer continues the operational data product⁶ currently provided by the Solar Backscatter Ultraviolet (SBUV/2) series of instruments on the Polar-orbiting Operational Environmental Satellites (POES). This paper provides a scientific overview of the nadir sensor and algorithm system, with an emphasis on the algorithm sensitivities to random and systematic sensor errors.

2. SCIENTIFIC BASIS AND HERITAGE

Ozone absorbs ultraviolet radiation beginning around 360 nm in the Huggins bands and increasing with decreasing wavelength down to 255 nm, at the peak of the Hartley absorption continuum⁷ (Fig. 1). The depletion of stratospheric ozone by man-made substances such as chlorofluorocarbons (CFCs) consequently results in an increase in near- and middle-ultraviolet solar radiation reaching the Earth's surface. The backscatter ultraviolet remote sensing technique uses Earth radiance and solar irradiance measurements from space to determine the amount of ozone absorption as a function of wavelength in this spectral range and hence the total column amount as well as the stratospheric ozone profile. The technique was first proposed in 1957⁸ and was subsequently placed on a firm theoretical basis⁹. The backscattered earth radiance increases by nearly five orders of magnitude between 250 and 380 nm (Fig. 2) due to the increase in the solar irradiance as well as decreasing ozone absorption. This dynamic range presents a challenge to instrument designers to achieve usable signal-to-noise ratios as well as to meet the demanding ~1% out-of-band rejection requirement across this spectral range.

* jrodrigu@ball.com; phone 1.303.939.6331; Ball Aerospace & Technologies Corp., 1600 Commerce Street, Boulder, CO 80301

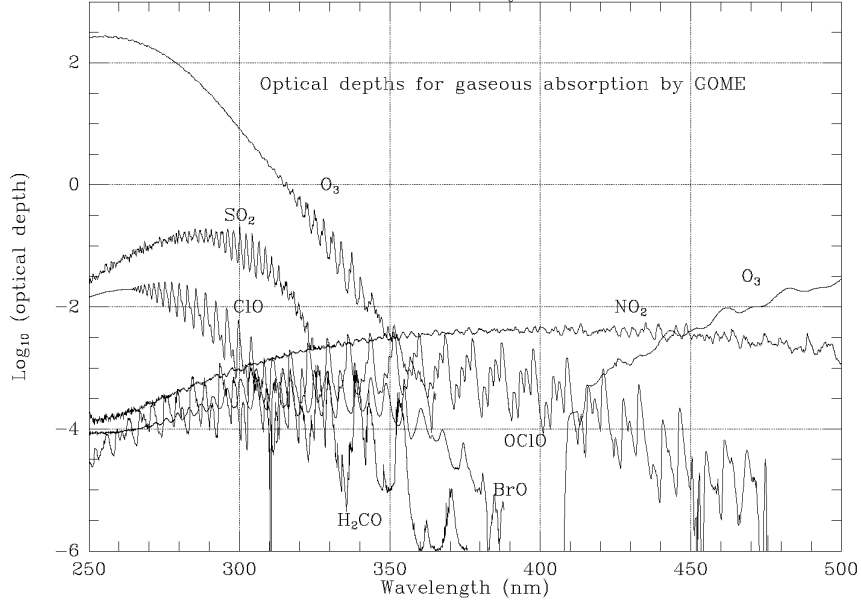


Figure 1: Absorption optical depths for trace gases in the 250-500 nm range and a typical measurement geometry line-of-sight. Enhanced conditions for SO₂ (volcanic) and OClO (ozone hole) are assumed. The backscatter ultraviolet technique for retrieving ozone total column uses radiance measurements in the Huggins bands below 360 nm, while the strong Hartley absorption between 250 and 310 nm provides information on the stratospheric ozone profile. The ozone Chappuis bands longward of 400 nm are used by the OMPS limb sensor to measure the ozone peak in the lower stratosphere. The OMPS nadir profile and total column spectrometers provide continuous spectral coverage between 250 and 310 nm and between 300 and 380 nm, respectively.

Following several space-borne experiments during the 1960's, the Backscatter Ultraviolet (BUV)¹¹ instrument was launched on April 8, 1970 on Nimbus 4. A direct ancestor of the current operational SBUV/2 series, the BUV included a double Ebert-Fastie monochromator (1.0 nm bandpass) that made measurements at twelve discrete wavelengths between 255 and 340 nm, and a separate filter photometer (5.0 nm bandpass) at 380 nm. These wavelengths enable both profile and total column retrievals based on the altitude contribution to radiances at each wavelength (Fig. 3). Similar wavelengths have been used on the Atmosphere Explorer E BUV¹³, the Nimbus 7 Solar Backscatter Ultraviolet (SBUV) radiometer¹⁴ and the NOAA SBUV/2 series¹⁵ to the present day. These double monochromators meet the demanding out-of-band requirement. The SBUV V6 algorithm⁶ is the baseline for OMPS nadir profile retrievals, which use discrete wavelengths selected from the complete spectrum provided by the double-pass nadir profile spectrometer³.

The total column algorithm^{16,17} developed for the BUV mission forms the basis for the algorithms used with the series of Total Ozone Mapping Spectrometers (TOMS) flown in space since 1978¹⁴ as well as the OMPS total column algorithm. The instrument measures both the Earth radiance I_j and the solar irradiance F_j at wavelengths j . The associated N-value

$$N_j = -100 \log_{10} (I_j / F_j) = -100 \log_{10} A_j$$

is a function of solar zenith angle, satellite zenith angle, ozone amount, and the reflectivity of the cloud-ground-aerosol surface observed at the non-ozone-absorbing wavelengths (e.g., 380 nm). Two N-values are paired, one at which ozone absorbs weakly and one at which ozone absorbs relatively strongly (but not so strongly that the surface cannot be seen). For example, the pair N-value for 312 and 336 nm is given by

$$N_p = N_{318} - N_{336} = 100 \log_{10} \left(\frac{A_{336}}{A_{318}} \right) = 43.43 \ln \left(\frac{A_{336}}{A_{318}} \right).$$

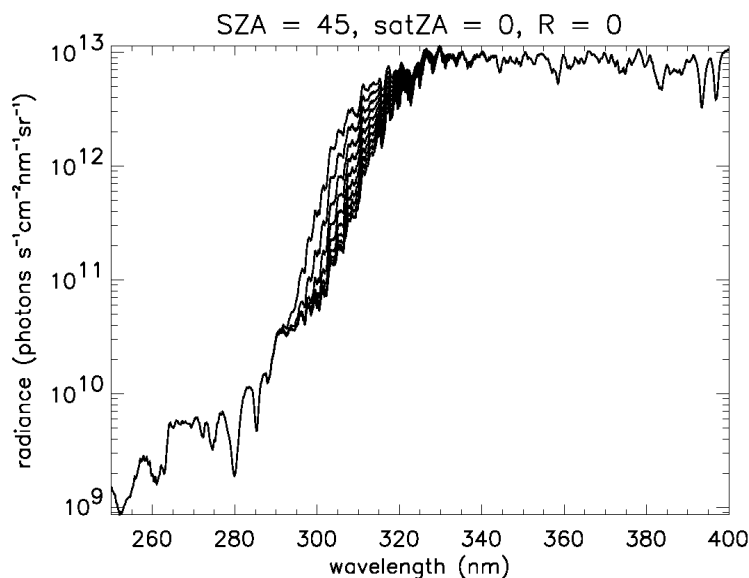


Figure 2: Backscatter ultraviolet radiance spectrum from 250 to 400 nm predicted using TOMRAD and a model solar spectrum, for ten TOMS standard model⁹ column amounts between 125 DU and 575 DU. (1 Dobson Unit or DU = 1 milli-atm-cm.) A decrease in ozone from 575 to 125 DU (ozone hole conditions) increases the 300-320 nm radiance by an order of magnitude. According to radiative transfer simulations, the corresponding UV-B radiation at the surface shows a similar increase under cloud-free conditions¹⁰.

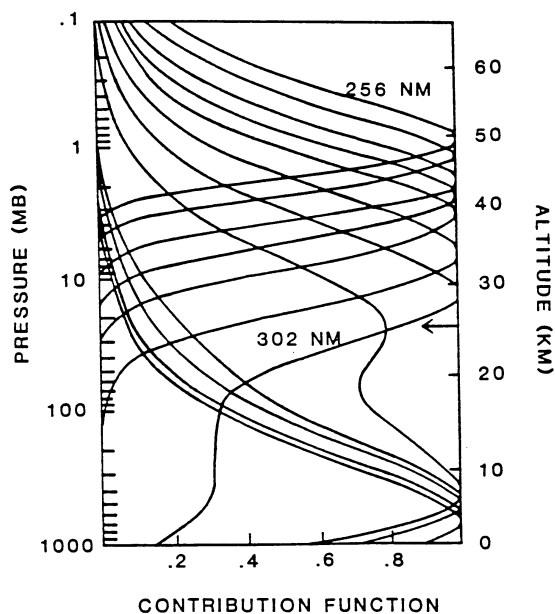


Figure 3: Single-scatter contribution functions for the Nimbus 7 SBUV monochromator wavelengths (255.7-339.9 nm). The six wavelengths with single-peaked contribution functions above 30 km (255.7-297.6 nm) due to ozone absorption are sensitive to the ozone profile. The four wavelengths with single-peaked contribution functions below 10 km (312.6, 317.6, 331.3, and 339.9 nm) due to Rayleigh scatter are sensitive to total column. The intermediate wavelengths (302.0 and 305.9 nm), with two peaks or a peak and a plateau in the contribution function, provide information on the total column and on the density-weighted mean altitude⁶. Similar wavelengths are used by the OMPS nadir profile algorithm. (After Fleig et al.¹²)

Using a technique that dates back to the BUVA algorithm¹⁷, the OMPS total column algorithm calculates an initial estimate of ozone using the 318 and 336 nm wavelength pair. This calculation uses an ozone sensitivity that is a linear interpolation from the radiative transfer tables. The initial estimate is given by

$$\Omega_0 = \Omega_L + \frac{N_{meas} - N_L}{dN_p/d\Omega}$$

where the N-values here are pair N-values, $dN_p/d\Omega$ is the ozone sensitivity given by

$$\frac{dN_p}{d\Omega} \approx \frac{N_U - N_L}{\Omega_U - \Omega_L}$$

and the subscripts U and L correspond to the upper and lower ozone amounts in the radiative transfer look-up tables corresponding to the pair N-values, N_L and N_U , that bracket the measured pair N-value N_{meas} at the observed solar zenith angle, satellite zenith angle, and azimuth angle and for calculated reflectivity. For a slant path s and a differential ozone absorption coefficient $\Delta\alpha$, the Beer's law approximation for this sensitivity is given by:

$$\frac{dN_p}{d\Omega} = 43.43s\Delta\alpha$$

In a plot of pair N-values as a function of total ozone for different wavelength pairs¹⁸, the pair N-value ozone sensitivities are the local slopes of these curves. The OMPS wavelength pair N-values (Fig. 4) are calculated from the OMPS master radiative transfer tables. The steepest slopes correspond to wavelength pairs with larger differential absorption between the two wavelengths. However, as the column amount increases, the slopes of the curves for the most sensitive pairs decrease and even go negative, indicating that the lowest wavelength no longer sees the surface.

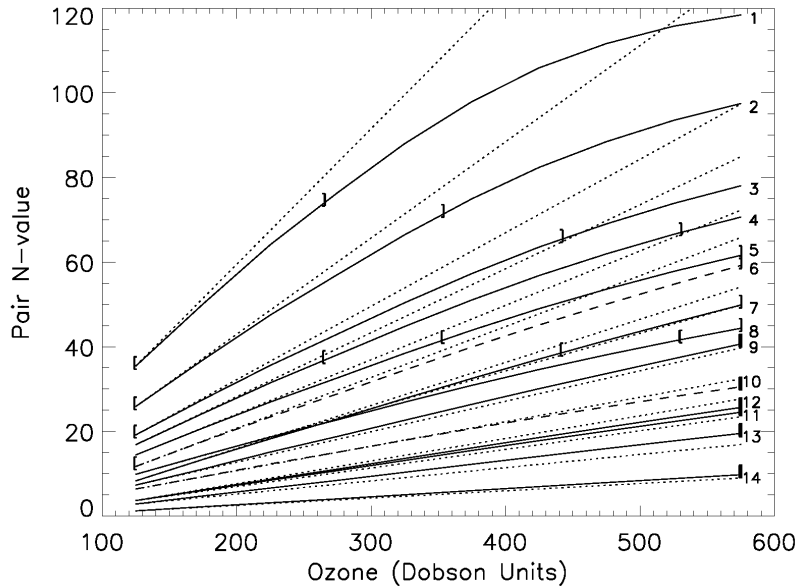


Figure 4: OMPS pair N-values for SZA = 45 deg, satellite ZA = 45 deg, azimuth = 0 deg, R = 0.2 at a pressure of 1.0 atm. Slant path = 2.83. The fourteen wavelength pairs are listed by Seftor et al⁴. (Pair 1 is 308.5 and 321.0 nm; pair 14 is 331.0 and 336.0 nm.) The solid curves are determined from the OMPS master radiative transfer table for each OMPS wavelength pair (the dashed curves are the special temperature-sensitive OMPS pairs). The dotted curves have the slope of sensitivities derived from Beer's law.

A key innovation in the TOMS V7 algorithm¹⁹ is the use of wavelength triplets to correct for differences between the measured and calculated N-values attributed to geophysical phenomena not included in the radiative transfer calculations (e.g., wavelength dependences in the modeled surface reflectivity) as well as to sensor characterization errors (e.g., sensor scattered light). This linear correction, applied simultaneously to both ozone-sensitive wavelengths, results in a retrieved total column value that is a small correction to the initial estimate Ω_0 :

$$\Omega = \Omega_0 + \frac{r_1(\lambda_2 - \lambda_R) - r_2(\lambda_1 - \lambda_R)}{\eta_1(\lambda_2 - \lambda_R) - \eta_2(\lambda_1 - \lambda_R)}$$

where the residue r_i is the difference between the measured and calculated N-value at absorbing wavelength i , η_i is the ozone sensitivity at wavelength i , and λ_R is the reflectivity wavelength. This approach has been generalized in the OMPS total column algorithm by using twelve triplets (three ozone-sensitive wavelength pairs with four reflectivity wavelengths) for the retrieval in each scene⁴.

3. TOTAL COLUMN SENSITIVITY TO SENSOR RANDOM ERRORS

Based on the above expression for retrieved ozone, the ozone error due to noise in the measured N-value is (in units of ozone):

$$\sigma_\Omega = \frac{43.43\sqrt{(\lambda_2 - \lambda_R)^2 e_1^2 + (\lambda_1 - \lambda_R)^2 e_2^2}}{|(\lambda_2 - \lambda_R)\eta_1 - (\lambda_1 - \lambda_R)\eta_2|}$$

where e_n is the normalized standard deviation of the normalized radiance random noise. Single wavelength sensitivities are often expressed in units of percent normalized radiance per percent ozone. In this form, they are given by:

$$\hat{\eta} = \frac{dA_\lambda / A_\lambda}{d\Omega / \Omega} = -\frac{\Omega}{43.43} \frac{dN_\lambda}{d\Omega}$$

Sensitivity expressed in terms of normalized radiance is negative since (for ozone sensitive wavelengths) the normalized radiance decreases as ozone increases. The single-triplet noise can therefore be rewritten as:

$$\frac{\sigma_\Omega}{\Omega} = \frac{\sqrt{(\lambda_2 - \lambda_R)^2 e_1^2 + (\lambda_1 - \lambda_R)^2 e_2^2}}{|(\lambda_2 - \lambda_R)\hat{\eta}_1 - (\lambda_1 - \lambda_R)\hat{\eta}_2|}$$

which is useful for estimating percent ozone error due to sensor random noise.

The TOMS instruments measure six wavelengths, from which three wavelength triplets are assembled by the TOMS V7 algorithm, each of which is used for a different optical path length ($s\Omega$) regime. By providing continuous spectral coverage between 300 and 380 nm, the OMPS total column spectrometer permits the OMPS total column algorithm to use fifty-six wavelength triplets. The pair N-value sensitivities (expressed as percent change in normalized radiance per percent change in ozone, or $s\Omega\Delta\alpha$ under the Beer's law assumption) used in the OMPS retrievals vary only about a factor of two over the required ozone measurement range and illumination conditions for solar zenith angles less than 80 degrees⁴.

An example using only six of the OMPS triplets (Table 1) shows how the random error due to sensor noise is kept within a fairly narrow range (Fig. 5). A signal-to-noise ratio (SNR) of 1000 is assumed for all wavelengths. Conditions representative of the darkest and brightest scenes have been modeled for two solar zenith angle cases. A single-triplet retrieval is assumed in each scene. The solar zenith angles (SZAs) vary realistically across the 110 degree field-of-

view. The predicted retrieval noise levels for the $\text{SZA} < 60$ deg cases are similar, indicating that the sensor and algorithm system achieve similar sensitivities across a wide range of ozone amounts, satellite zenith angles, and solar zenith angles. The cases for higher SZAs show larger errors, with the error being largest for edge of scan ($\text{SZA} = 80$ deg), but, again, similar sensitivities are achieved within this SZA range across a wide range of ozone amounts and satellite zenith angles. With the twelve separate optical path length ($s\Omega$) regimes provided by the complete set of OMPS triplets and the twelve triplets used in each retrieval, the sensitivity jumps shown in Figure 5 will be reduced by the OMPS total column algorithm. At this level, the sensor noise contribution to the overall OMPS total column precision ($3 \text{ DU} + 0.5\%$ of column) is relatively small⁴.

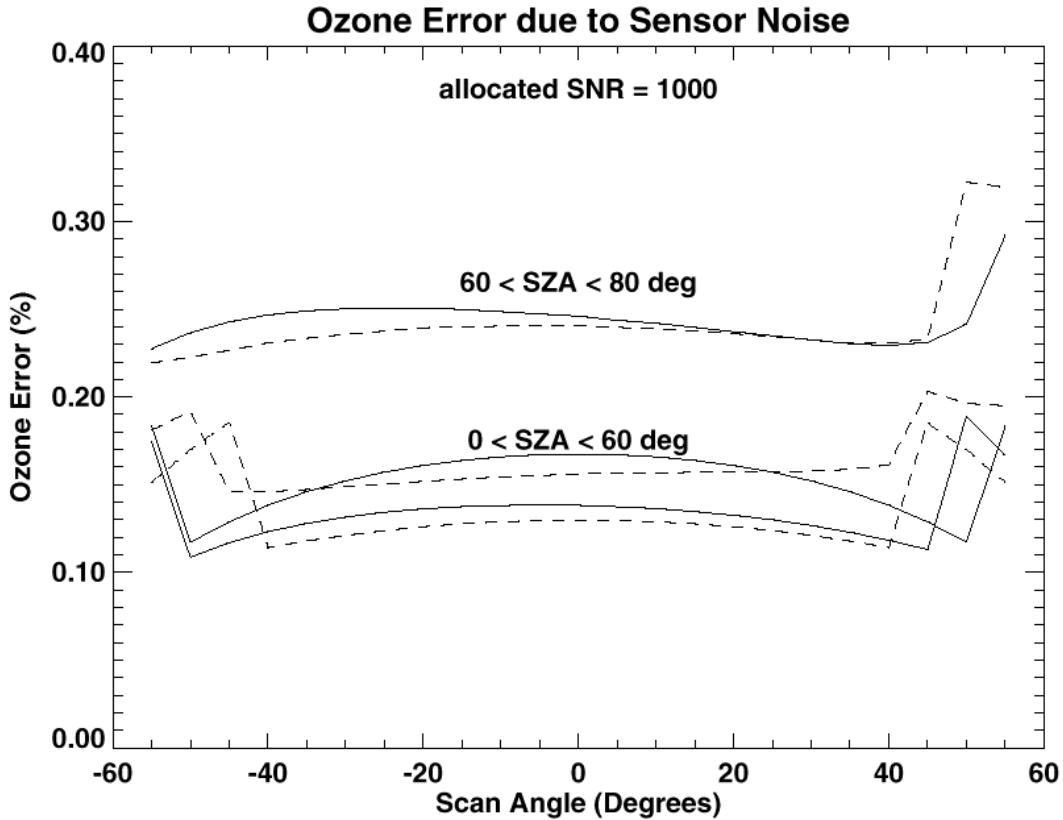


Figure 5: Ozone error due to sensor SNR = 1000 for a wide range of scenes. The “scan angle” axis represents the ± 55 deg field-of-view of the OMPS nadir telescope. The solid curves represent bright cases (low ozone, cloudy scene) while the dashed curves represent dark cases (high ozone, clear scene). The curves for $0 < \text{SZA} < 60$ deg include two cases for low SZA and two cases for moderate SZA. The cases for low SZA are $\Omega = 300 \text{ DU}$, $R = 0$ and $\Omega = 200 \text{ DU}$, $R = 1$. The cases for moderate SZA are $\Omega = 450 \text{ DU}$, $R = 0.2$ and $\Omega = 200 \text{ DU}$, $R = 1$. The two curves for $60 < \text{SZA} < 80$ deg represent $\Omega = 75 \text{ DU}$, $R = 1$ and $\Omega = 650 \text{ DU}$, $R = 0$.

Table 1: OMPS wavelength triplets used in Figure 5.

λ_1 (nm)	λ_2 (nm)	λ_R (nm)	Optical Path Range
308.5	321.0	377.0	$s\Omega < 0.75$
312.5	321.0	377.0	$0.75 < s\Omega < 1.0$
314.0	321.0	377.0	$1.0 < s\Omega < 1.75$
318.0	336.0	377.0	$1.25 < s\Omega < 2.5$
322.0	332.0	377.0	$2.5 < s\Omega < 5.0$
328.0	336.0	377.0	$3.5 < s\Omega$
331.0	336.0	377.0	$5.0 < s\Omega$

4. TOTAL COLUMN SENSITIVITY TO OUT-OF-BAND SCATTERED LIGHT

In the TOMS and OMPS total column algorithms, the residues are the difference between the measured and calculated N-values at ozone-absorbing wavelengths. The OMPS wavelength triplet algorithm corrects for any linear variation in the N-values residues with wavelength. Consequently, any deviation from the assumed linear variation represents an uncorrected error. Since N-value is approximately linear with ozone over a wide range of viewing conditions (Fig. 4), this percent error in normalized radiance translates directly to an error in retrieved ozone. Out-of-band scattered light is an example of a sensor error that may result in residues that are non-linear in wavelength.

Figure 6 schematically represents the percentage change in normalized radiance ($A = I/F$) caused by scattered light for a wavelength triplet. In this figure, λ_3 represents the reflectivity wavelength and λ_1 and λ_2 represent the ozone-sensitive wavelength pair. The terms $(\beta_A/A)_1$, $(\beta_A/A)_2$, and $(\beta_A/A)_3$ represent the percent error in normalized radiance for wavelength 1, wavelength 2, and wavelength 3, respectively, where β represents a systematic error in a quantity such as radiance and $(\beta_A/A) = (\beta_I/I) - (\beta_F/F)$. Any normalized radiance change that is linear in wavelength is corrected by the algorithm. Furthermore, since λ_1 is the only one of the three wavelengths strongly sensitive to ozone, only deviations of λ_1 from the line drawn between λ_2 and λ_3 result in an ozone error. The deviation of the residue $(\beta_A/A)_1$ from the straight line due to scattered light at λ_1 is:

$$\text{deviation} = \left(\frac{\beta}{A} \right)_1 - \left(\frac{\lambda_3 - \lambda_1}{\lambda_3 - \lambda_2} \right) \left[\left(\frac{\beta}{A} \right)_2 - \left(\frac{\beta}{A} \right)_3 \right]$$

The overall error due to scattered light (e_Ω) can then be written as:

$$e_\Omega \propto \left(\frac{\beta}{A} \right)_1 - \left(\frac{\lambda_3 - \lambda_1}{\lambda_3 - \lambda_2} \right) \left[\left(\frac{\beta}{A} \right)_2 - \left(\frac{\beta}{A} \right)_3 \right] - \left(\frac{\beta}{A} \right)_3$$

where the term $(\beta/A)_3$ represents an overall error due to scattered light. (This error is equivalent to a wavelength-independent calibration error, or an error in the calibration baseline, which affects the reflectivity determined from the radiance at λ_3 .) Analysis using the TOMS A triplet (312, 321, and 364 nm) indicates that for a 3 DU error in ozone, the percent deviation in the 312 nm wavelength can be no greater than 0.8%. Similar studies using the TOMS B and C triplets and their worst case viewing conditions indicate that the deviation must be less than 0.5% and 0.3%, respectively, to meet the 3 DU allocation.

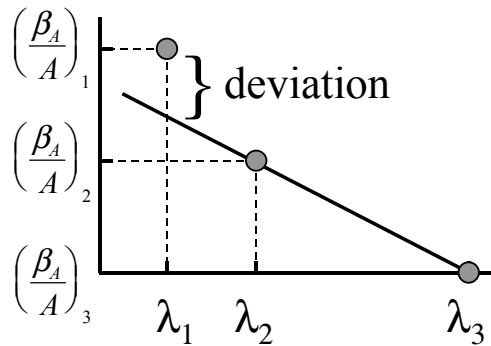


Figure 6: Geometric interpretation of the scattered light error as corrected by the wavelength triplet formulation developed for TOMS V7 and adapted for OMPS. Ozone is determined from the wavelength pair λ_1 and λ_2 , and reflectivity is determined from the ozone-insensitive wavelength λ_3 . The terms $(\beta_A/A)_1$, $(\beta_A/A)_2$, and $(\beta_A/A)_3$ represent the percent error in normalized radiance for λ_1 , λ_2 , and λ_3 , respectively. A normalized radiance change that is linear in wavelength is corrected by the algorithm. Only deviations of the ozone-sensitive wavelength λ_1 from the line drawn between λ_2 and λ_3 contribute to ozone error.

Figure 7 shows model calculations of the nadir sensor's radiance scattered light as a function of wavelength for 225 and 325 DU atmospheres. This range of total column amounts represents most cases observed in the tropics. The calculation assumes the presence of a spectral flattening filter³ and a characteristic grating scatter model. Superimposed on this figure are two lines (one corresponding to the 225 DU response and one to the 325 DU response) drawn through the 321 and 364 nm wavelengths and extending out to 312 nm. The deviation of the 312 nm response from the straight line is 0.2% at 225 DU and 0.3% at 325 DU. That is, the deviation for both cases is well below the 0.8% required to meet the 3 DU error allocation.

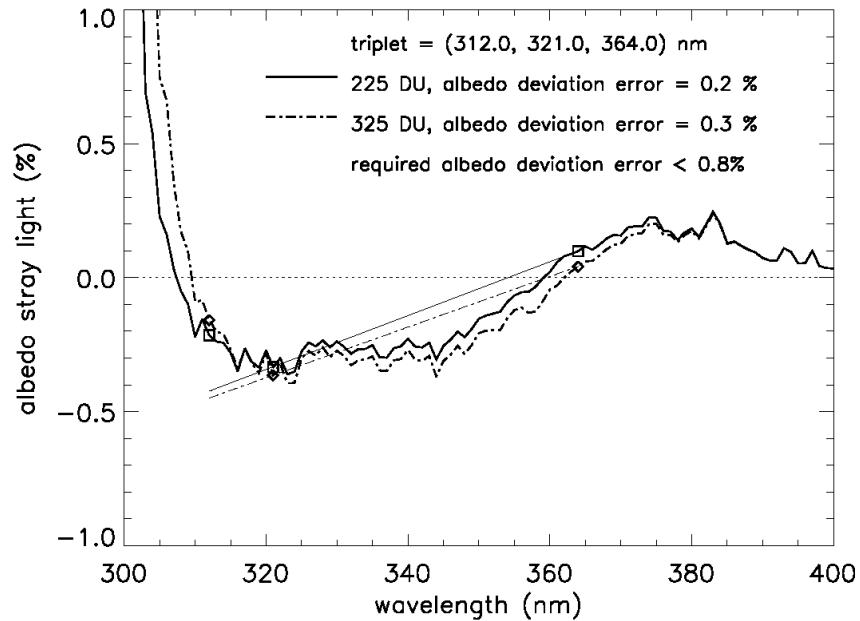


Figure 7: Normalized radiance or albedo scattered light (β_A/A) predicted for the nadir sensor and the deviation errors calculated for 225 DU and 325 DU, SZA = 0, satellite ZA = 0, and R = 0. The lines connect normalized radiance values for $\lambda_2 = 321.0$ and $\lambda_3 = 364.0$ nm, analogous to Figure 6. The deviation from this line at $\lambda_1 = 312$ nm is the normalized radiance deviation error.

5. ADDITIONAL DATA PRODUCTS FROM THE OMPS NADIR SENSOR

In addition to the operational total column and nadir profile environmental data records (EDRs), the OMPS nadir sensor and algorithm system will produce sensor data records (SDRs) containing calibrated and geolocated spectral radiances that can be used to derive other data products off-line. The total column spectrometer reports a complete 300-380 nm spectrum every 7.6 seconds (50 km at nadir) in thirty-five nearly equiangular cross-track cells across the 2800 km swath. The nadir profile spectrometer reports a complete 250-310 nm spectrum every 38 seconds in a single 250 x 250 km cell at nadir. The two spectrometers are coregistered in order to provide the 310-380 nm range to the nadir profiling algorithm. Both spectra are sampled at 0.42 nm centers using charge-coupled device array detectors, resulting in 192 channels reported for total column and 145 channels reported for nadir profile. The spectral resolution of each channel is 1.0 nm FWHM.

TOMS-like data by-products from the OMPS total column algorithm include tropospheric ozone, effective cloud fraction, scene reflectivity, the aerosol index, and the volcanic sulfur dioxide index. As with TOMS radiances²⁰, OMPS SDRs can be used to derive aerosol optical depth. As an example of additional data products that can be derived from OMPS nadir SDRs, we consider measurements of trace gases that have significant and structured absorption between 300 and 380 nm that can be resolved at 1.0 nm FWHM resolution. These include formaldehyde (HCHO), bromine monoxide (BrO), chlorine dioxide (OCIO), nitrogen dioxide (NO₂), and sulfur dioxide (SO₂) (Fig. 1). The candidate species have all been measured by the Global Ozone Monitoring Experiment (GOME); this sensitivity study includes

direct experience in analyzing GOME measurements to produce realistic estimates. Table 2 shows the spectral ranges for the measurements, the maximum and minimum expected signal-to-noise ratios for OMPS total column spectrometer measurements (for the ozone horizontal cell sizes), and one-sigma sensitivities for vertical column amounts of the species for single OMPS observations. The sensitivities are derived directly from the cross sections used in analysis of GOME spectra. The expected minimum and maximum SNR for the OMPS roughly correspond to high-albedo and low-albedo (ocean) conditions. Systematic effects, chiefly the ability to quantitatively model spectral features, currently limit the ability to fit for trace gas columns to several parts in 10^4 of the measured radiance. This limit, which is now readily achieved in retrievals from individual GOME spectra, is applied to the following discussions of sensitivities for individual molecules.

Table 2: Trace gas measurements that could be derived from OMPS total column SDRs

Molecule	Spectral Range (nm)	Max/Min SNR*	Vertical Sensitivity, Max SNR (mol-cm ²)	Vertical Sensitivity, Min SNR (mol-cm ²)
HCHO	336-357	5300/2700	6.76E+14	1.33E+15
BrO	345-369	6500/2200	4.12E+12	1.22E+13
OCIO	354-383	7400/1800	4.83E+12	1.98E+13
NO ₂	340-380	6000/2250	1.38E+14	3.69E+14
SO ₂	313-327	6000/2500	4.94E+14	1.18E+15

* predicted at the OMPS Preliminary Design Review

Formaldehyde (HCHO)

Formaldehyde is fundamental to tropospheric oxidation processes and therefore is an indicator of anthropogenic pollution and biomass burning. Vertical column measurements over land and water from OMPS should be limited by systematic modeling effects to about $1.3\text{E}+15$ molecules/cm² at minimum SNR. HCHO vertical columns at low-and-mid-latitudes range from $3\text{E}+14$ to $1\text{E}+16$ molecules/cm² and even higher under conditions of heavy biomass burning. Formaldehyde can now be retrieved robustly from GOME observations²¹.

Bromine monoxide (BrO)

Bromine monoxide (BrO) strongly influences stratospheric ozone and is listed under the highest priority of controlling species by multiple international panels on atmospheric observations. It has recently been shown to be influential in the destruction and moderation of tropospheric ozone in polar spring conditions. BrO measurements have been demonstrated extensively and are now made readily from all GOME measurements²². Operational processing for global BrO is currently under development.

Chlorine dioxide (OCIO)

Chlorine dioxide (OCIO) is an excellent indicator of a perturbed stratosphere. From experience with GOME, where robust measurements of OCIO are readily made²³, OCIO is measurable by OMPS in the polar vortex where the Antarctic ozone hole occurs, to the same precision as GOME. Measurements to SNR of 10 or greater can be made for ozone hole concentrations. It may be possible to determine OCIO outside the vortex to modest accuracy. Limitation of the OMPS wavelength range to 380 nm does not significantly effect the measurement of OCIO.

Nitrogen dioxide (NO₂)

Nitrogen dioxide (NO₂) is involved in both stratospheric ozone chemistry and tropospheric pollution caused by anthropogenic production. NO₂ measurements from OMPS will be limited in accuracy, compared to GOME and other instruments, because of the 380 nm long-wavelength cutoff of the OMPS measurement range. GOME measures NO₂ at 425-450 nm, where the depth of structures in the NO₂ spectrum is significantly greater than for the region covered by the OMPS total column spectrometer. OMPS will provide significant measurements of NO₂, with a lower limit due to systematic fitting effects near the sensitivity at minimum SNR, or about $3\text{E}+14$ to $4\text{E}+14$ cm⁻² vertical column NO₂. The largest atmospheric columns (seen, for example, in biomass burning events and from urban pollution) approach the $1\text{E}+16$ cm⁻² level, and can readily be mapped by OMPS. Clean air background levels are near the measurement sensitivity of OMPS, and can thus only be measured with significant precision in summed measurements at degraded spatial resolution.

Sulfur dioxide (SO₂)

Sulfur dioxide (SO₂) has now been measured by GOME²⁴ from volcanic production and from pollution in the U.S., Eastern Europe, and China. Current work is underway to determine how well background SO₂ column amounts can be characterized. Vertical columns from volcanic production can exceed 15 DU, or 4E+17 cm⁻² (1 DU = 2.69E+16 cm⁻²), and a very polluted troposphere can have in excess of 5 DU (background amounts are less than 1 DU). GOME measurements are currently limited by instrument-specific systematic effects. The ability of OMPS to measure SO₂ should be better than what has been accomplished with GOME (0.04 DU with worst-case SNR), permitting extensive global measurements of both volcanic SO₂ production and anthropogenic pollution.

6. CONCLUSIONS

The OMPS nadir sensor and algorithm system represents the next generation in U. S. operational ozone total column mapping. This system, combining a new sensor design with EDR algorithms based on over 40 years of research and development, will continue the ozone data record currently produced by the TOMS and SBUV/2 series of instruments. The complete 250-380 nm spectral radiances produced by the sensor and SDR algorithms will permit the retrieval of trace gases using techniques already proven with GOME. Measuring natural and anthropogenic trace gases that affect ozone chemistry will complement the long-term ozone monitoring that is one of the primary missions of OMPS.

7. ACKNOWLEDGMENTS

This work was supported by the NPOESS Integrated Program Office under contracts F04701-97-C0032 and F04701-99-C044 and by Ball Aerospace & Technologies Corp. OMPS is the result of many years of work by dedicated personnel from government, academia, and industry.

8. REFERENCES

1. C. S. Nelson and J. D. Cunningham, The National Polar-orbiting Operational Environmental Satellite System future U.S. environmental observing system, *Proceedings of the American Meteorological Society 82nd Annual Meeting*, paper 3.1, January 2002.
2. J. Hornstein, E.P. Shettle, R.M. Bevilacqua, S. Chang, E. Colon, L. Flynn, E. Hilsenrath, S. Mango, H. Bloom, and F. Sanner, The Ozone Mapping and Profiler Suite-Assimilation Experiment (OMPS-AE), IGARSS, II:809-812 2002.
3. M. Dittman et al., Nadir ultraviolet imaging spectrometer for the NPOESS Ozone Mapping and Profiler Suite (OMPS), *Proc. SPIE*, 4814, 2002.
4. C. J. Seftor, J. C. Larsen, T. J. Swissler, J. V. Rodriguez, Q. Remund, G. Jaross, and C. G. Wellemeyer, OMPS total column algorithm performance: comparison to TOMS and to NPOESS requirements, *Proc. SPIE*, 4891, 2002.
5. M. Dittman et al., Limb broad-band imaging spectrometer for the NPOESS Ozone Mapping and Profiler Suite (OMPS), *Proc. SPIE*, 4814, 2002.
6. P. K. Bhartia, R. D. McPeters, C. L. Mateer, L. E. Flynn, and C. Wellemeyer, Algorithm for the estimation of vertical ozone profiles from the backscattered ultraviolet technique, *J. Geophys. Res.*, 101, 18,793-18,806, 1996.
7. R. E. Huffman, *Atmospheric Ultraviolet Remote Sensing*, Academic Press, 320 pp., 1992.
8. S. F. Singer and R. C. Wentworth, A method for the determination of the vertical ozone distribution from a satellite, *J. Geophys. Res.*, 62, 299-308, 1957.
9. C. G. Wellemeyer, S. L. Taylor, C. J. Seftor, R. D. McPeters, and P. K. Bhartia, A correction for total ozone mapping spectrometer profile shape errors at high latitudes, *J. Geophys. Res.*, 102, 9029-9038, 1997.
10. D. F. Heath and Z. Ahmad, Applications of ultraviolet absolute radiometry in satellite and surface based remote sensing of atmospheric ozone, *Proc. SPIE*, 4482, 94-103, 2002.
11. D. F. Heath, C. I. Mateer, and A. J. Krueger, The Nimbus-4 backscatter ultraviolet (BUV) atmospheric ozone experiment – two years' operation, *PAGEOPH*, 106-108, 1239-1253, 1973.
12. A. J. Fleig, R. D. McPeters, P. K. Bhartia, B. M. Schlesinger, R. P. Cebula, K. F. Klenk, S. L. Taylor, and D. F. Heath, *Nimbus 7 Solar Backscatter Ultraviolet (SBUV) Ozone Products User's Guide*, NASA Ref. Pub. 1234, 1990.

13. J. E. Frederick, R. B. Abrams, R. Dasgupta, and B. Guenther, Natural variability of tropical upper stratospheric ozone inferred from the Atmosphere Explorer Backscatter Ultraviolet experiment, *J. Atmos. Sci.*, 38, 1092-1099, 1981.
14. D. F. Heath, A. J. Krueger, H. A. Roeder, and B. D. Henderson, The solar backscatter ultraviolet and total ozone mapping spectrometer (SBUV/TOMS) for NIMBUS G, *Opt. Eng.*, 14, 323-331, 1975.
15. Z. Ahmad et al., Accuracy of total ozone retrieval from NOAA SBUV/2 measurements: impact of instrument performance, *J. Geophys. Res.*, 99, 22,975-22,984, 1994.
16. J. V. Dave and C. L. Mateer, A preliminary study on the possibility of estimating total atmospheric ozone from satellite measurements, *J. Atmos. Sci.*, 24, 414-427, 1967.
17. C. L. Mateer, D. F. Heath, and A. J. Krueger, Estimation of total ozone from satellite measurements of backscattered ultraviolet Earth radiance, *J. Atmos. Sci.*, 28, 1307-1311, 1971.
18. J. V. Dave, Effect of aerosols on the estimation of total ozone in an atmospheric column from the measurement of its ultraviolet radiance, *J. Atmos. Sci.*, 35, 899-911, 1978.
19. R. D. McPeters et al., *Nimbus-7 Total Ozone Mapping Spectrometer (TOMS) Data Products User's Guide*, NASA Ref. Pub. 1384, 1996.
20. O. Torres, P. K. Bhartia, J. R. Herman, A. Sinyuk, P. Ginoux, and B. Holben, A long-term record of aerosol optical depth from TOMS observations and comparison to AERONET measurements, *J. Atmos. Sci.*, 59, 398-413, 2002.
21. P. I. Palmer, D. J. Jacob, K. Chance, R. V. Martin, R. J. D. Spurr, T. P. Kurosu, I. Bey, R. Yantosca, A. Fiore, and Q. Li, Air mass factor formulation for spectroscopic measurements from satellites: application to formaldehyde retrievals from the Global Ozone Monitoring Experiment, *J. Geophys. Res.*, 106, 14,539-14,550, 2001.
22. K. Chance, Analysis of BrO measurements from the Global Ozone Monitoring Experiment, *Geophys. Res. Lett.*, 25, 3335, 1998.
23. T. Wagner, C. Leue, K. Pfeilsticker, and U. Platt, Monitoring of the stratospheric chlorine activation by Global Ozone Monitoring Experiment (GOME) OCIO measurements in the austral and boreal winters 1995 through 1999, *J. Geophys. Res.*, 106, 4971-4986, 2001.
24. M. Eisinger and J.P. Burrows, Tropospheric sulfur dioxide observed by the ERS-2 GOME instruments, *Geophys. Res. Lett.*, 25, 4177-4180, 1998.